

## Layered Double Hydroxide/Chitosan Composite (Mg-Al/CT) as a Selective Adsorbent in Congo Red Adsorption from Aqueous Solution

Risfidian Mohadi<sup>1</sup>, Patimah Mega Syah Bahar Nur Siregar<sup>2</sup>,  
Neza Rahayu Palapa<sup>3</sup>, Tarmizi Taher<sup>4</sup>, Aldes Lesbani<sup>1,3\*</sup>

<sup>1</sup> Graduate School of Faculty Mathematics and Natural Sciences, Sriwijaya University, Jl. Padang Selasa No. 524 Ilir Barat 1, Palembang-South Sumatera, Indonesia

<sup>2</sup> Magister Program, Faculty Mathematics and Natural Sciences, Sriwijaya University, Jl. Padang Selasa No. 524 Ilir Barat 1, Palembang-South Sumatera, Indonesia

<sup>3</sup> Research Center of Inorganic Materials and Complexes, Faculty of Mathematics and Natural Sciences, Sriwijaya University, Jl. Padang Selasa Bukit Besar Palembang 30139, South Sumatera, Indonesia

<sup>4</sup> Departement of Environmental Engineering, Faculty of Mathematics and Natural Sciences, Insitut Teknologi Sumtera, Jl. Terusan Ryacudu, Way Hui, Jati Agung, Lampung 35365, Indonesia

\* Corresponding author's e-mail: [aldeslesbani@pps.unsri.ac.id](mailto:aldeslesbani@pps.unsri.ac.id)

### ABSTRACT

Layered double hydroxide (LDH) can be used as an adsorbent to remove pollutants from aqueous solutions, but it drawbacks where the structure is easily damaged so that it cannot be reused in the adsorption process and has a low adsorption capacity. This can be overcome through the development of layered double hydroxide material composited with chitosan support material. In addition to utilizing waste, chitosan is selected as supporting material in the layered double hydroxide modification process, because it is cheap, has high selectivity, and is biodegradable. In this study, the adsorbent was applied in the process of removing Congo Red (CR). The LDH modification process using chitosan was successfully carried out, as seen from XRD analysis which resembled the base material (Mg-Al) and support (CT), the BET analysis which showed an increase in surface area, as well as from the large adsorption capacity value and the regeneration process which tends to be stable after compositing is done.

**Keywords:** adsorption, Congo Red, modified of layered double hydroxide, regeneration.

### INTRODUCTION

Color is the first recognized contaminant in wastewater. The waste generated from the use of these dyes can have a serious impact on humans and other living things (Elmoubarkia et al., 2017). Congo Red (CR) is a type of red azo dye that is commonly found in the textile industry (Zhang et al., 2018). Congo Red has the chemical formula  $C_{32}H_{22}N_6Na_2O_6S_2$  with the structure sodium ben-zidindiazo-bis-1-naphthylamine-4-sulfonate in it. Congo Red has a molecular weight of 696.665 g/mol (Vinsiah et al., 2017) (Fig. 1).

Several methods can be used to remove dyes, such as biological treatment, coagulation (Banerjee & Chattopadhyaya, 2017), photocatalysis (Kaur et al., 2021), and adsorption (Wang et al., 2020). The adsorption method is a reliable alternative because it is easy to operate (Ali et al., 2020), simple (Noreena et al., 2020), available for various adsorbents, and has high efficiency (Zhang et al., 2019). Several factors can affect the adsorption process, such as adsorbate concentration, effect of temperature, contact time, surface area from material, and particle size (Sonia et al., 2020).

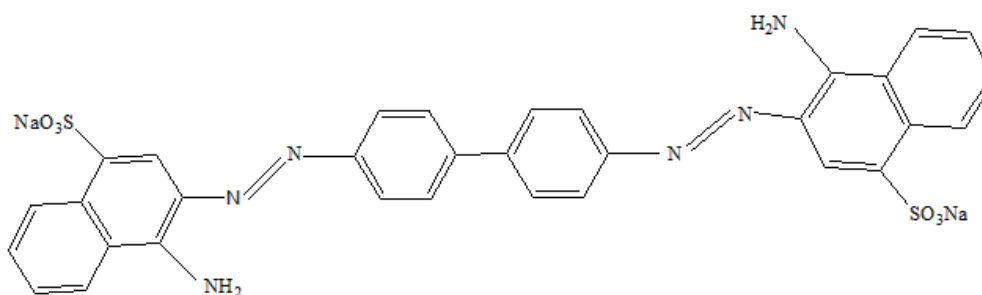


Figure 1. Congo Red

Layered double hydroxide (LDH) can be used to adsorb anionic dyes but cannot be applied to cationic dyes, so it is necessary to modify the layered double hydroxide so that it can absorb various types of dyes. According to Wu et al., (2017) layered double hydroxide has limitations as an adsorbent to adsorb dyes and its repeated use is not effective. Layered double hydroxide can be modified with composites. Supporting materials that can be used in the layered double hydroxide modification process include activated carbon, graphite, biochar, hydrochar, and chitosan (Pietrelli et al., 2014).

Chitosan (CT) is environmentally friendly, inexpensive, has good stability, and abundant availability, which makes it widely used in the layered double hydroxide modification process (Barkhordari & Alizadeh, 2021). Chitosan is used in the adsorption process of pollutants in aqueous solution (Zhang et al., 2016). Chitosan is an organic compound containing  $\text{NH}_2$  and  $-\text{OH}$  groups in its molecular structure so it can be used as an adsorbent in the adsorption process (Dey et al., 2016; Muinde et al., 2020). Chitosan can be extracted from the shells of shrimp, crab, clams, and lobster (Mulyani et al., 2019).

The adsorption capacity of 2,4-dichlorophenol from 1.33 mg/g to 1.96 mg/g after modification of layered double hydroxide (Co-Fe) using chitosan (Yang et al., 2018). Layered double hydroxide Mn-Fe material composited with chitosan could be used repeatedly to remove indigo carmine dye, as seen from the regeneration process which did not experience a significant decrease in four consecutive cycles of 98.80%; 91.07%; 81.29% and 64.37% (Khalili et al., 2021).

In this work, Mg-Al was modified using chitosan as supporting material. The Mg-Al/CT composite was applied for CR dye removal. The synthesized material was then analyzed using XRD, FTIR, and BET. In this research, the selectivity process for mixed dyestuffs was carried out first, followed by kinetics, thermodynamics, and regeneration studies.

## EXPERIMENT

### Chemicals and instrumentations

In this research, materials include  $\text{Mg}(\text{NO}_3)_2 \cdot 6\text{H}_2\text{O}$  (256.41 g/mol),  $\text{Al}(\text{NO}_3)_3 \cdot 9\text{H}_2\text{O}$  (375.13 g/mol), chitosan extracted from shrimp shells through demineralization and deproteination process, distilled water from PT. Bratachem Indonesia, NaOH (40 g/mol), Congo Red (CR), Methylene Blue (MB), Malachite Green (MG), and Rhodamine-B (Rh-B). The materials were characterized using XRD analysis from Rigaku Miniflex-6000, FTIR from Shimadzu Prestige-21. UV-Visible Bio-Base spectrophotometer BK-UV1800 was used to measure dye concentration.

### Preparation of Mg-Al

Mg-Al can be synthesized using the coprecipitation method;  $\text{Mg}(\text{NO}_3)_2 \cdot 6\text{H}_2\text{O}$  solution (19.23 g, 100 mL) and  $\text{Al}(\text{NO}_3)_3 \cdot 9\text{H}_2\text{O}$  solution (9.378 g, 100 mL) were mixed (Badri et al., 2021). The Mg-Al mixture was added with NaOH (2 M) until the pH of the solution was 10 and stirred at 80°C for 24 hours. After stirring is complete, the precipitate is filtered and rinsed using distilled water. The precipitate was dried and the resulting solid was characterized using XRD, FTIR, and BET analysis.

### Preparation of chitosan

Extraction of chitosan from shrimp shells can be carried out by demineralization and deproteination processes (Mohadi et al., 2021). The demineralization process was carried out by smoothing the shrimp shells and putting 100 g of the finely chopped shrimp shells were placed into beaker, then HCl was added a ratio of 1:10 (w/v). The mixture was stirred at 60°C for 3 hours. After completion, the mixture was filtered and the residue dried at 70 °C. The demineralized residue was put into

beaker and NaOH was added with a similar ratio. The mixture was stirred for 1 hour at 60 °C. The mixture was then filtered and the precipitate was dried at 70°C. The chitosan obtained was characterized using XRD, FTIR, and BET analysis.

### Preparation of Mg-Al/CT

The Mg-Al/CT preparations were made by the coprecipitation method (Elanchezhian & Meenakshi, 2017). Total of 15 mL (0.75 M) Mg solution and 15 mL (0.25 M Al solution). The solution was mixed and adjusted the pH to 10 using 2 M NaOH then the mixture was stirred for 1 hour. After the stirring process is complete, 3 g of chitosan is added and then stirred for 72 hours at 80°C. The precipitate was dried and characterized using XRD, FTIR, and BET analysis.

### Selectivity of dyes

20 mg/L (CR, Rh-B, MG, and MB) as much as 10 mL, added 0.02 g of adsorbent, then stirred with variations of time (0, 15, 30, 60, and 120 minutes) and the adsorbed was measured using a UV-Vis spectrophotometer.

### Kinetic study

20 mL of CR solution (200 mg/L, 0.02 g adsorbent), then stirred with various contact times (0, 10, 20, 30, 60, 90, 120, 150, 180, 200, and 250 minutes). After the stirring is complete, the Congo Red solution and the adsorbent were separated using centrifugation. The filtrate was measured at the maximum wavelength of Congo Red (466 nm) using a UV-Visible spectrophotometer.

### Adsorption process

The adsorption process was carried out using variations in CR concentration (60–100 mg/L) and adsorption temperature (30–60°C). Then the filtrate was measured at the maximum wavelength of CR (466 nm) using a UV-Visible spectrophotometer.

### Regeneration

The regeneration process was carried out by adsorption of 25 mL CR dye (100 mg/L, 1 g adsorbent). After the adsorption process was completed, measurements were conducted using a UV-Vis spectrophotometer. Then the adsorbent containing

the dye was desorbed using an ultrasonic device. After completion, the adsorbent was dried using an oven and continued with the adsorption process with the same procedure for seven cycles.

## RESULTS AND DISCUSSION

The sharp peaks of Mg-Al shown in Figure 2(a) angles  $2\theta = 11.47^\circ(003)$ ,  $22.86^\circ(006)$ ,  $34.69^\circ(009)$ , and  $61.62^\circ(110)$  indicating Mg-Al has a high crystal structure similar to the research conducted by (Bolbol et al., 2019). The widened peaks defined as amorphous peaks of chitosan at angles of  $2\theta = 7.93^\circ$  and  $19.35^\circ$  with plane reflections (002) and (006) are shown in

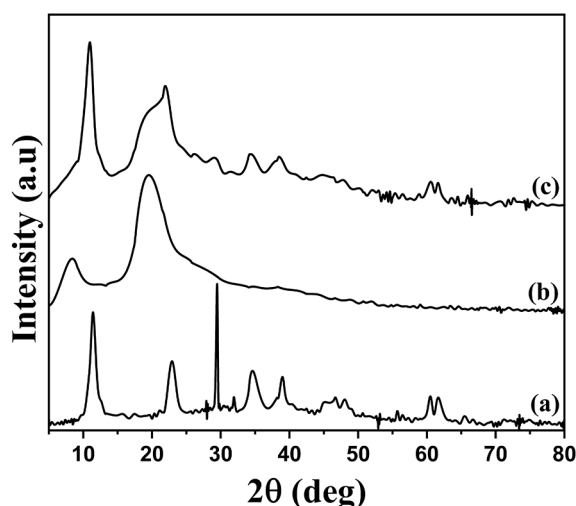


Figure 2. XRD analysis of Mg-Al (a), CT (b), Mg-Al/CT (c)

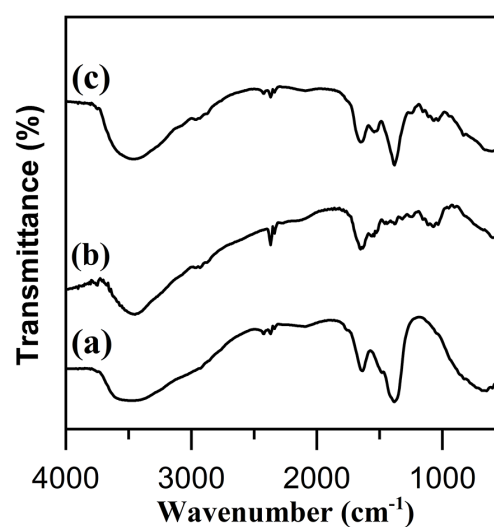


Figure 3. FTIR analysis of Mg-Al (a), CT (b), Mg-Al/CT (c)

Figure 2(b). The diffraction pattern of Mg-Al/CT is shown in Figure 2(c). Figure 2(c) shows the same peaks as Mg-Al and chitosan diffraction, namely  $10.83^\circ(003)$ ,  $19.52^\circ(006)$ , and  $60.6^\circ(110)$  (Li et al., 2006).

Figure 3 shows the FTIR spectrum of each material. Vibration peaks associated with stretching  $\text{NH}_2$  and OH groups appear at wavenumber  $3447\text{ cm}^{-1}$ . The peak at wavenumber  $1657\text{ cm}^{-1}$  was associated with the  $\text{CONH}_2$  group of chitosan (Kumar & Koh, 2012). The peak that appears at wavenumber  $1381\text{ cm}^{-1}$  indicates the presence of  $\text{NO}_3^-$  anion vibrations from LDH (Shabanian et al., 2020). The FTIR spectrum synthesized is similar to that reported by Chen et al., (2017) with different absorption intensities.

The BET analysis of each material is shown in Figure 4. It confirms that each material follows a type IV isotherm with hysteresis loop. The type IV isotherm indicates that the adsorption and desorption patterns of the material do not overlap. The hysteresis loop indicates that the material has mesopores (Siregar et al., 2021). Layered double hydroxide (Mg-Al) has a surface area of  $8.963\text{ m}^2/\text{g}$ , chitosan (CT) has a surface area of  $3.288\text{ m}^2/\text{g}$ ,

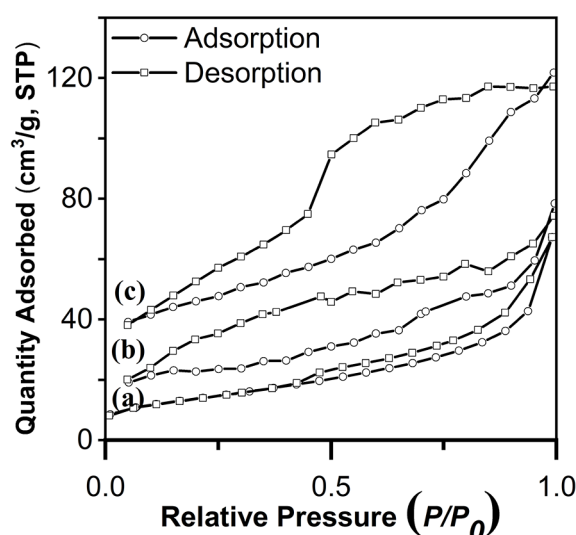


Figure 4. BET analysis of Mg-Al (a), CT (b), and Mg-Al/CT (c)

Table 1. BET analysis of materials

| Materials | Surface area ( $\text{m}^2/\text{g}$ ) | Pore volume ( $\text{cm}^3/\text{g}$ ) BJH | Pore size (nm), BJH |
|-----------|--|--|---------------------|
| Mg-Al     | 8.963                                  | 0.027                                      | 3.169               |
| CT        | 3.288                                  | 0.006                                      | 6.092               |
| Mg-Al/CT  | 24.556                                 | 0.027                                      | 3.929               |

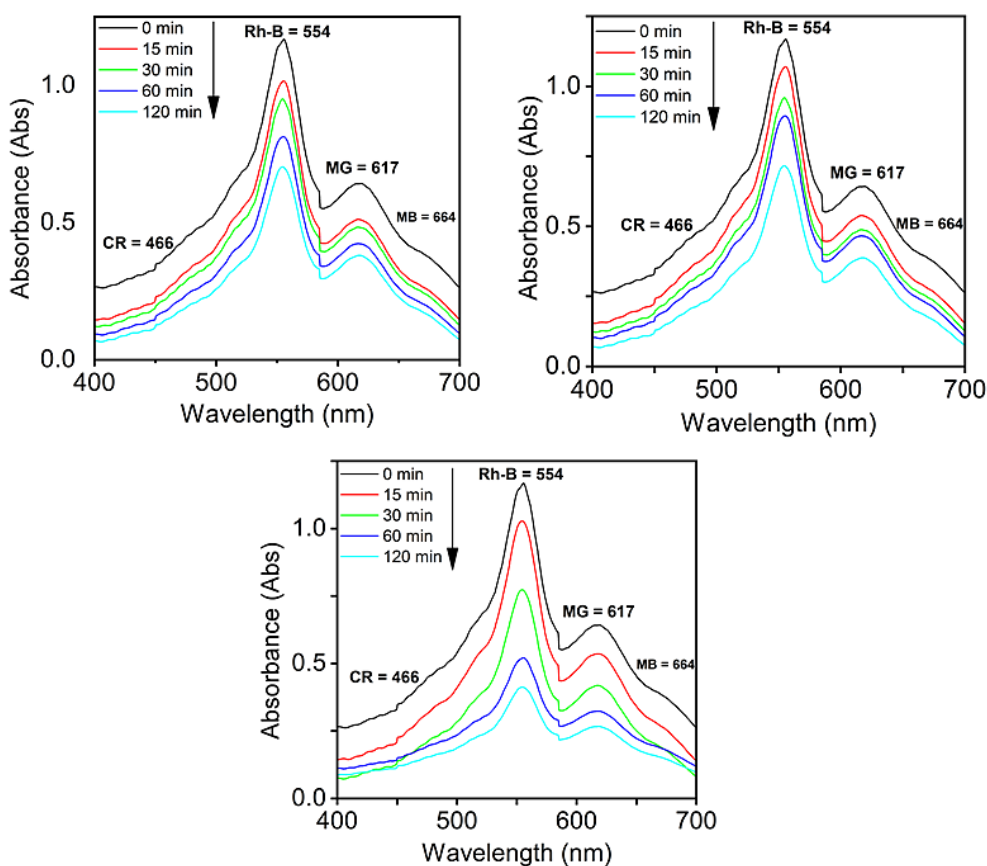


Figure 5. Selectivity of dyes mixture CR, Rh-B, MG and MB with variation contact time onto Mg-Al (a), CT (b), and Mg-Al/CT (c)

**Table 2.** Kinetic parameter

| Adsorbent | $Q_{e\_exp}$ (mg/g) | PFO                  |       |       | PSO                  |       |        |
|-----------|---------------------|----------------------|-------|-------|----------------------|-------|--------|
|           |                     | $Q_{e\_Calc}$ (mg/g) | $R^2$ | $k_1$ | $Q_{e\_Calc}$ (mg/g) | $R^2$ | $k_2$  |
| Mg-Al     | 81.061              | 87.720               | 0.907 | 0.016 | 101.010              | 0.991 | 0.0002 |
| CT        | 70.833              | 83.869               | 0.965 | 0.018 | 93.458               | 0.991 | 0.0001 |
| Mg-Al/CT  | 117.803             | 120.837              | 0.876 | 0.015 | 128.205              | 0.951 | 0.0001 |

$m^2/g$ , and Mg-Al/CT composites have a surface area of  $24.556 m^2/g$  shown in Table 1. The Mg-Al/CT composites showed the largest surface area compared to their constituent materials (Mg-Al and CT). This confirmed that the Mg-Al modification process using chitosan was successfully carried out.

The dye mixtures (CR, Rh-B, MG, and MB) were measured at a wavelength of 400–700 nm (Figure 5). The graph of the selectivity of the dye mixture shows that with increasing adsorption time, the absorbance obtained also decreases. At the 120 minutes, there was a significant decrease in absorbance and it was seen that CR had the most significant decrease in absorbance compared to other dyes. Then the CR dye was carried out by adsorption processes such as

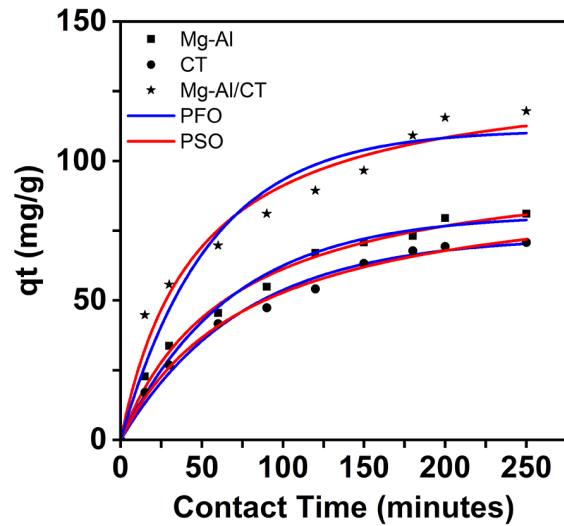


Figure 6. Adsorption contact time

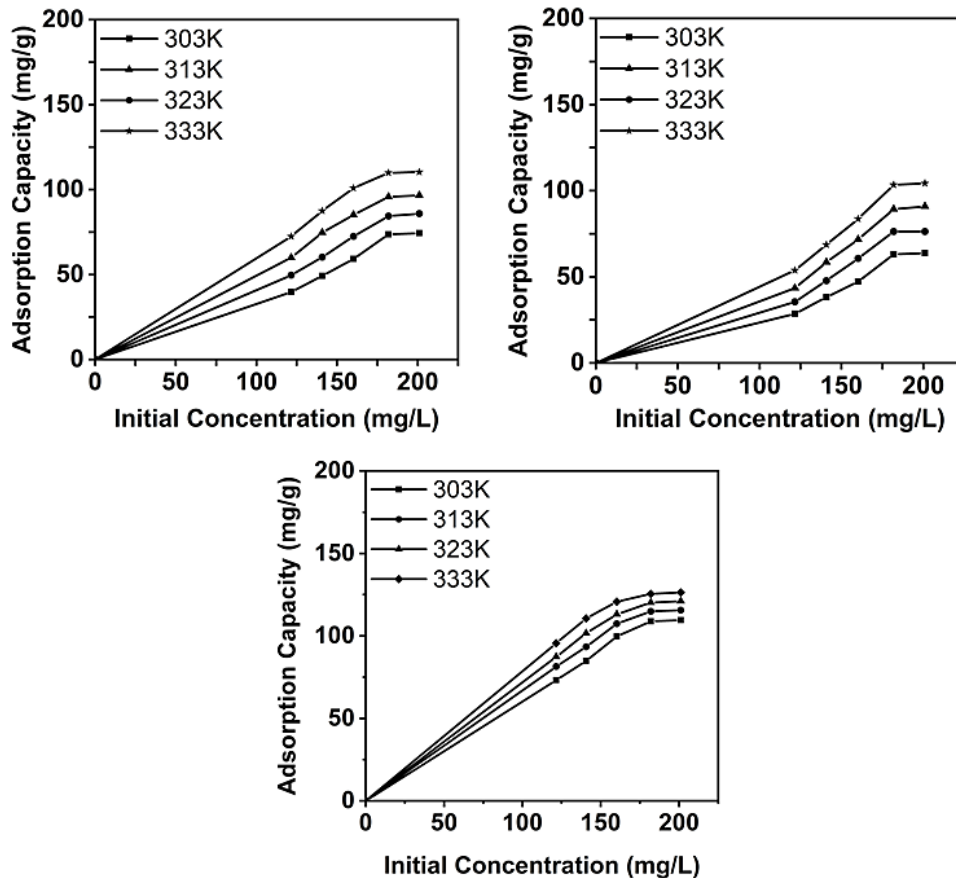


Figure 7. Effect of adsorption on Mg-Al (a), CT (b), Mg-Al/CT (c)

from the influence of contact time, isotherm, thermodynamics, and regeneration.

Figure 6 shows the optimum contact time at 200 minutes, under optimum conditions there was an increase in the maximum absorption of the dye or the equilibrium rate of adsorption so that the addition of time had no significant effect. Table 2 shows the adsorption kinetics of each adsorbent tends to follow Pseudo Second Order (PSO) which is indicated by the value of  $R^2$  which is close to 1 and the value of  $k_2$ , which indicates the adsorption process is faster in Pseudo Second Order. and the difference in theoretical and

experimental  $Q_e$  values in Pseudo Second Order is not significant (Guechi & Hamdaoui, 2016).

The maximum adsorption process occurred at 333 K and at 120 minutes as shown in Figure 7.

The suitable isotherm model can be determined by looking at the data of the coefficient of determination ( $R^2$ ). If the  $R^2$  value is closer to 1, it can be said that there is a greater influence and the relationship between variables stronger. Table 3 shows that the  $R^2$  value tends to follow the Freundlich equation, which means that the absorption of Congo Red occurs by physisorption (physical absorption). Physical adsorption occurs because

**Table 3.** Isotherm adsorption

| Adsorbent | Adsorption Isotherm | Adsorption Constant | T (K)   |         |         |         |
|-----------|---------------------|---------------------|---------|---------|---------|---------|
|           |                     |                     | 303     | 313     | 323     | 333     |
| Mg-Al     | Langmuir            | Qmax                | 46.083  | 84.746  | 63.694  | 120.482 |
|           |                     | kL                  | 0.006   | 0.005   | 0.152   | 0.008   |
|           |                     | $R^2$               | 0.981   | 0.951   | 0.938   | 0.835   |
|           | Freundlich          | n                   | 0.464   | 0.563   | 1.066   | 0.582   |
|           |                     | kF                  | 3.410   | 3.991   | 1.471   | 1.090   |
|           |                     | $R^2$               | 0.987   | 0.994   | 0.998   | 0.973   |
| CT        | Langmuir            | Qmax                | 39.216  | 53.476  | 67.568  | 116.279 |
|           |                     | kL                  | 0.005   | 0.005   | 0.006   | 0.005   |
|           |                     | $R^2$               | 0.972   | 0.985   | 0.944   | 0.975   |
|           | Freundlich          | n                   | 0.330   | 0.267   | 0.248   | 0.277   |
|           |                     | kF                  | 3.331   | 4.861   | 9.307   | 7.705   |
|           |                     | $R^2$               | 0.975   | 0.999   | 0.984   | 0.995   |
| Mg-Al/CT  | Langmuir            | Qmax                | 192.308 | 222.222 | 263.158 | 344.828 |
|           |                     | kL                  | 0.025   | 0.032   | 0.014   | 0.067   |
|           |                     | $R^2$               | 0.798   | 0.899   | 0.907   | 0.956   |
|           | Freundlich          | n                   | 1.821   | 2.151   | 2.606   | 3.426   |
|           |                     | kF                  | 13.005  | 21.198  | 18.728  | 23.361  |
|           |                     | $R^2$               | 0.792   | 0.838   | 0.832   | 0.829   |

**Table 4.** Thermodynamic adsorption

| Adsorbent | T (K) | $Q_e$ (mg/g) | $\Delta H$ (kJ/mol) | $\Delta S$ (J/mol K) | $\Delta G$ (kJ/mol) |
|-----------|-------|--------------|---------------------|----------------------|---------------------|
| Mg-Al     | 303   | 74.427       | 20.058              | 0.070                | -1.151              |
|           | 313   | 85.878       |                     |                      | -1.851              |
|           | 323   | 96.565       |                     |                      | -2.551              |
|           | 333   | 110.305      |                     |                      | -3.251              |
| CT        | 303   | 63.740       | 23.643              | 0.080                | -0.564              |
|           | 313   | 76.336       |                     |                      | -1.363              |
|           | 323   | 90.840       |                     |                      | -2.162              |
|           | 333   | 104.198      |                     |                      | -2.961              |
| Mg-Al/CT  | 303   | 129.779      | 22.875              | 0.080                | -1.503              |
|           | 313   | 141.687      |                     |                      | -2.308              |
|           | 323   | 153.901      |                     |                      | -3.112              |
|           | 333   | 161.382      |                     |                      | -3.917              |

of physical forces (Siregar et al., 2021). The physically adsorbed molecules are not strongly bound to the surface of the adsorbent, and usually, a fast reversible process occurs, so they are easy to replace with other molecules. The value of ( $n > 1$ ) indicates a physical adsorption process (Rath et al., 2019). The respective adsorption capacities of Congo Red are shown in Table 3. The maximum adsorption capacities obtained using Mg-Al, CT, and Mg-Al/CT were 120.482 mg/g, 116.279 mg/g, 344.828 mg/g, respectively, as shown in Table 3.

Table 4 shows the thermodynamic data of adsorption using Mg-Al, CT, and Mg-Al/CT. Positive enthalpy value data ( $\Delta H$ ) indicates that the adsorption process is endothermic. The data of entropy or degree of disorder ( $\Delta S$ ) that occurs during adsorption on each adsorbent shows a small value. The greater the concentration of Congo Red, the smaller the degree of adsorption irregularity. Gibbs free energy data ( $\Delta G$ ) shows a negative value which indicates the adsorption process occurs spontaneously for each adsorbent (Siregar et al., 2021).

The Mg-Al/CT regeneration process showed an insignificant decrease for seven different cycles with Mg-Al and CT as shown in Figure 8. This shows that Mg-Al/CT is a good adsorbent in the process of adsorption of CR, this is evidenced by the increased surface area after the composite process, greater adsorption capacity, and better structural stability than Mg-Al and CT.

Table 5 shows the comparison of Congo Red absorption using various adsorbents. The Congo

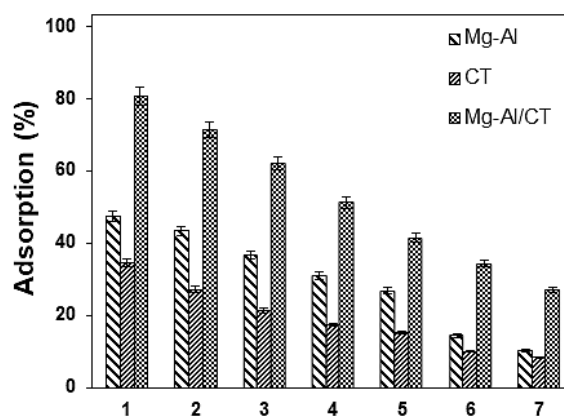


Figure 8. Regeneration cycle of each adsorbent

Red adsorption capacity obtained in this study is greater than the adsorbent in Table 5.

## CONCLUSIONS

The manufacturing of composites based on layered double hydroxide (Mg-Al) and support material of chitosan (CT) were successfully synthesized. The success of material synthesis was proven by the results of XRD, FTIR, and BET analysis. XRD analysis showed the Mg-Al has typical peaks at angles of  $2\theta = 11.47^\circ$  (003),  $22.86^\circ$  (006),  $34.69^\circ$  (009), and  $61.62^\circ$  (110) and peaks of chitosan appear at angles of  $2\theta = 7.93^\circ$  (002) and  $19.35^\circ$  (006). The results of BET analysis showed that the surface area of Mg-Al was  $8.963 \text{ m}^2/\text{g}$  and increased after modifying layered double hydroxide with chitosan to  $24.556 \text{ m}^2/\text{g}$ . Adsorption parameters were studied through

Table 5. Adsorption of CR from aqueous solutions using several adsorbent

| Adsorbent                   | Adsorption capacity (mg/g) | Reference                 |
|-----------------------------|----------------------------|---------------------------|
| Metal hydroxides sludge     | 40                         | (Attallah et al., 2013)   |
| Diatomaceous Earth          | 23.2                       | (Sriram et al., 2020)     |
| Shiitake mushroom           | 217.86                     | (Yang et al., 2020)       |
| <i>Aspergillus Niger</i>    | 3.805                      | (Hamad & Saied, 2021)     |
| Bread fruit seed shell      | 16                         | (Conrad et al., 2016)     |
| TiO <sub>2</sub> /SCEC      | 18.4                       | (Widiyowati et al., 2020) |
| ZnO/chitosan                | 227.3                      | (Nguyen et al., 2020)     |
| Magnetic chitosan composite | 181.82                     | (Wang et al., 2013)       |
| Na bentonite                | 35.84                      | (Vimonsesa et al., 2009)  |
| Kaolin                      | 5.44                       | (Vimonsesa et al., 2009)  |
| Zeolit                      | 3.77                       | (Vimonsesa et al., 2009)  |
| Mg-Al                       | 120.482                    | This study                |
| CT                          | 116.279                    | This study                |
| Mg-Al/CT                    | 344.828                    | This study                |

variations in contact time, isotherm, and thermodynamics. The kinetic model of each adsorbent tends to follow the pseudo second order (PSO). The isotherm data for each adsorbent shows that the adsorption isotherm model tends to follow the Freundlich isotherm. The adsorption capacity of Mg-Al is 120.482 mg/g, chitosan is 116.279 mg/g, and Mg-Al/CT is 344.828 mg/g. Mg-Al/CT is the most effective adsorbent for adsorption of congo red repeatedly seen from the regeneration cycle which did not experience a significant decrease in adsorption capacity for seven cycles.

### Acknowledgments

All authors thanks the Laboratory of Inorganic Materials and Complexes of the Faculty of Mathematics and Natural Sciences, Sriwijaya University for support of this research.

### REFERENCES

1. Ali F., Bibi S., Ali N., Ali Z., Said A., Wahab Z.U., Bilal M., Iqbal H.M.N. 2020. Sorptive removal of malachite green dye by activated charcoal: Process optimization, kinetic, and thermodynamic evaluation. *Case Studies in Chemical and Environmental Engineering*, 2, 1–5. <https://doi.org/10.1016/j.cscee.2020.100025>
2. Badri A.F., Siregar P.M.S.B.N., Palapa N.R., Mohadi R., Mardiyanto M., Lesbani A. 2021. Mg-Al/Biochar Composite with Stable Structure for Malachite Green Adsorption from Aqueous Solutions. *Bulletin of Chemical Reaction Engineering & Catalysis*, 16(1), 149–160. <https://doi.org/10.9767/brec.16.1.10270.149-260>
3. Banerjee S., Chattopadhyaya M. 2017. Adsorption characteristics for the removal of a toxic dye, tartrazine from aqueous solutions by a low cost agricultural by-product. *Arabian Journal of Chemistry*, 10, 1629–1638. <https://doi.org/10.1016/j.arabjc.2013.06.005>
4. Barkhordari S., Alizadeh A. 2021. Fabrication of pH-sensitive chitosan/layered double hydroxide (LDH)/Fe<sub>3</sub>O<sub>4</sub> nanocomposite hydrogel beads for controlled release of diclofenac. *Polymer Bulletin*, 0123456789, 1–16. <https://doi.org/10.1007/s00289-021-03761-3>
5. Bolbol H., Fekri M., Hejazi-Mehrizi M. 2019. Layered double hydroxide-loaded biochar as a sorbent for the removal of aquatic phosphorus: behavior and mechanism insights. *Arabian Journal of Geosciences*, 12(16), 1–11.
6. Chen Y.-X., Zhu R., Ke Q.-F., Gao Y.S., Zhang C.Q., Ya-Ping Guo Y.P. 2017. MgAl layered double hydroxide/chitosan porous scaffolds loaded with PFT $\alpha$  to promote bone regeneration. *Nanoscale*, 9(20), 6765–6776. <https://doi.org/10.1039/C7NR00601B>
7. Dey S.C., Al-Amin M., Rashid T.U., Sultan M.Z., Ashaduzzaman M., Sarker M., Shamsuddin S. M. 2016. Preparation, Characterization And Performance Evaluation Of Performance Evaluation Of Chitosan As An Adsorbent For Remazol Red. *International Journal of Latest Research in Engineering and Technology (IJLRET)*, 2(2), 55–62.
8. Elanchezhiyan S.S., Meenakshi S. 2017. Synthesis and characterization of chitosan/Mg-Al layered double hydroxide composites for the removal of oil particles from oil in water emulsion. *International Journal of Biological Macromolecules*, 104, 1586–1595. <https://doi.org/10.1016/j.ijbiomac.2017.01.095>
9. Elmoubarkia R., Mahjoubia F.Z., Elhalila A., Tounsadia H., Abdennouria M., Sadiqa M., Qourzalb S., Zouhric A., Barka N. 2017. Ni/Fe and Mg/Fe layered double hydroxides and their calcined derivatives : preparation, characterization and application on textile dyes. *Integrative Medicine Research*, 6(3), 271–283. <https://doi.org/10.1016/j.jmrt.2016.09.007>
10. Guechi E.K., Hamdaoui O. 2016. Sorption of malachite green from aqueous solution by potato peel : Kinetics and equilibrium modeling using non-linear analysis method. *Arabian Journal of Chemistry*, 9, 416–424. <https://doi.org/10.1016/j.arabjc.2011.05.011>
11. Kaur H., Singh S., Pal B. 2021. Environmental Nanotechnology , Monitoring & Management A brief review on modified layered double hydroxides for H<sub>2</sub> production through photoinduced H<sub>2</sub> O splitting. *Environmental Nanotechnology, Monitoring & Management*, 16, 100451. <https://doi.org/10.1016/j.enmm.2021.100451>
12. Khalili R., Ghaedi M., Parvinnia M., Mehdi M., Sabzehmeidan. 2021. Simultaneous removal of binary mixture dyes using mn - Fe layered double hydroxide coated chitosan fibers prepared by wet spinning. *Surface and Interfaces*, 23, 100976.
13. Kumar S., Koh J. 2012. Physicochemical, optical and biological activity of chitosan-chromone derivative for biomedical applications. *International Journal of Molecular Sciences*, 13(5), 6103–6116. <https://doi.org/10.3390/ijms13056102>
14. Li B., He J., Evans D.G., Duan X. 2006. Morphology and size control of Ni-Al layered double hydroxides using chitosan as template. *Journal of Physics and Chemistry of Solids*, 67, 1067–1070. <https://doi.org/10.1016/j.jpics.2006.01.027>
15. Mohadi R., Palapa N.R., Hartono R., Hidayati N., Rozirwan. 2021. The Utilization of Modified Chitosan from Shrimp Shell As Photodegradation of



- Pesticides Paraquat Dichloride. *Science and Technology Indonesia*, 6(3), 2–6.
16. Muinde V.M., Onyari J.M., Wamalwa B., Wabomba J.N. 2020. Adsorption of malachite green dye from aqueous solutions using mesoporous chitosan-zinc oxide composite material. *Environmental Chemistry and Ecotoxicology*, 2, 115–125. <https://doi.org/10.1016/j.enceco.2020.07.005>
  17. Mulyani R., Mulyadi D., Yusuf N. 2019. Preparation and Characterization of Chitosan Membranes from Crab Shells (*Scylla olivacea*) for Beverage Preservative. *Jurnal Kimia Valensi*, 5(2), 242–247. <https://doi.org/10.15408/jkv.v5i2.10637>
  18. Noreena S., Khalida U., Ibrahim S.M., Javed T., Ghanie A., Nazf S., Iqbal M. 2020. ZnO, MgO and FeO adsorption efficiencies for direct sky Blue dye: equilibrium, kinetics and. *Integrative Medicine Research*, 9(3), 5881–5893. <https://doi.org/10.1016/j.jmrt.2020.03.115>
  19. Pietrelli L., Francolinib I., Piozzib A. 2014. Dyes Adsorption from Aqueous Solutions by Chitosan. *Taylor & Francis*, 50(8), 37–41. <https://doi.org/10.1080/01496395.2014.964632>
  20. Rath P.P., Priyadarshini B., Behera S.S., Parhi P.K., Panda S.R., Sahoo T.R. 2019. Adsorptive removal of Congo Red dye from aqueous solution using TiO<sub>2</sub> nanoparticles : Kinetics, thermodynamics and isothermal insights Adsorptive removal of Congo Red Dye from aqueous solution using TiO<sub>2</sub> nanoparticles : Kinetics, Thermodynamics and Isot. *Applied Surface Science*, 257(5), 2–6.
  21. Shabanian M., Hajibeygi M., Raeisi A. 2020. FTIR characterization of layered double hydroxides and modified layered double hydroxides. *Layered Double Hydroxide Polymer Nanocomposites*, 77–102. <https://doi.org/10.1016/B978-0-08-101903-0.00002-7>
  22. Siregar P.M.S.B.N., Palapa N.R., Wijaya A., Fitri E.S., Lesbani A. 2021. Structural Stability of Ni/Al Layered Double Hydroxide Supported on Graphite and Biochar Toward Adsorption of Congo Red. *Science and Technology Indonesia*, 6(2), 85–95. <https://doi.org/10.26554/STI.2021.6.2.85-95>
  23. Sonia S., Bajpaib P.K., Mittal J., Arora C. 2020. Utilisation of Cobalt doped Iron based MOF for enhanced removal and recovery of methylene blue dye from waste water. *Journal of Molecular Liquids*, 314, 113642. <https://doi.org/10.1016/j.molliq.2020.113642>
  24. Vinsiah R., Mohadi R., Lesbani A. 2017. Performance of Graphite for Congo Red and Direct Orange Adsorption. *Indonesian Journal of Environmental Management and Sustainability*, 4(4), 125–132.
  25. Wang A., Sun X., Li B., Shang H., Jiang Y., Zhao Z. 2020. Preparation of Carbon-Iron Composites Materials and Studies of Its Adsorption Properties for the Methylene Blue. *Journal of Inorganic and Organometallic Polymers and Materials*, 31(3), 1293–1303. <https://doi.org/10.1007/s10904-020-01754-9>
  26. Wu H., Zhang H., Yang Q., Wang D., Zhang W., Yang X. 2017. Calcined Chitosan-Supported Layered Double Hydroxides : An Efficient and Recyclable Adsorbent for the Removal of Fluoride from an Aqueous Solution. *Materials*, 10, 2–18. <https://doi.org/10.3390/ma10111320>
  27. Yang B., Liu J., Liu Z., Wang Y., Cai J., Peng L. 2018. Preparation of chitosan/Co-Fe-layered double hydroxides and its performance for removing 2, 4-dichlorophenol. *Environmental Science and Pollution Research*, 26(4), 3814–3822.
  28. Zhang L., Zeng Y., Cheng Z. 2016. Removal of heavy metal ions using chitosan and modified chitosan: A review. *Journal of Molecular Liquids*, 214, 175–191. <https://doi.org/10.1016/j.molliq.2015.12.013>
  29. Zhang W., Liang Y., Wang J., Zhang Y., Gao Z., Yang Y., Yang K. 2019. Ultrasound-assisted adsorption of Congo Red from aqueous solution using Mg-Al-CO<sub>3</sub> layered double hydroxide. *Applied Clay Science*, 174, 100–109. <https://doi.org/10.1016/j.clay.2019.03.025>
  30. Zhang Z., Li Y., Du Q., Li Q. 2018. Adsorption of Congo Red from Aqueous Solutions by Porous Soybean Curd Xerogels. *Polish Journal of Chemical Technology*, 20(3), 95–102. <https://doi.org/10.2478/pjct-2018-0044>